Corrosion Durability and Structural Response of Functionally-Graded Concrete Beams

Mohamed Maalej[1], Shaikh F.U. Ahmed[2] and P. Paramasivam[3]

Received 4 March 2003, accepted 31 May 2003

Abstract

This paper reports the results of an experimental program on the effectiveness of a Ductile Fiber Reinforced Cementitious Composite (DFRCC) material, which exhibit strain-hardening and multiple-cracking bahavior under flexural loadings, in retarding the corrosion of steel in Reinforced Concrete (RC) beams. Based on the collective findings from theoretically-estimated steel losses, rapid chloride permeability tests, pH value tests, as well as structural tests, it was concluded that Functionally-Graded Concrete (FGC) beams, where a layer of DFRCC material was used around the main longitudinal reinforcement, had a noticeably higher resistance against reinforcement corrosion compared to a conventional RC beam. The better performance of the FGC beams was also evident from the absence of any corrosion-induced cracking and the very low tendency of the concrete cover to delaminate as measured by a concrete-embeddable fiber optic strain sensor.

1. Introduction

Different corrosion-protection techniques, namely the use of epoxy-coated steel bars, cathodic protection, corrosion-inhibiting admixtures and supplementary cementing materials (SCM) are currently being used to prevent the corrosion of steel in reinforced concrete (RC) structures caused by the penetration of aggressive substances into the concrete. Initially, the concrete cover acts as a physical barrier that impedes the penetration of aggressive substances into RC structures. Over time, however, the aggressive substances are able to penetrate and reach the steel reinforcement through the pores and existing cracks causing depassivation of the steel and initiation of corrosion. The volume and size of pores in the concrete can be reduced by making the concrete denser through the use, for instance, of pozzolanic materials (CANMET 1987; Mehta 1998; Mehta 1999). The width of load- and environmentally-induced cracks can also be controlled to some degree by proper selection of concrete material and proper distribution of the steel reinforcement in the concrete member. The study published by Tsukamoto and Worner (1990) suggests that the effective permeability of concrete (permeability of concrete in the presence of cracks) to aggressive substances can be significantly reduced by decreasing the crack width.

Current design codes specify crack width limits at the tensile face of reinforced concrete structures as function of exposure conditions (ACI Committee 224 1991; ACI Committee 318 1999; CEB 1993). However, the crack width limits specified for an aggressive environment are so low that it is nearly impossible or at least impractical to achieve in practice using conventional steel reinforcement and commonly-used concrete. In addition, when these limits are used in conjunction with the recommended equations for controlling crack widths, it is expected that a portion of the cracks in a structure will exceed these values by a significant amount (ACI Committee 224 1991). To address this limitation, Maalej and Li (1995) proposed a new design for RC flexural members. The design consisted of replacing part of the concrete which surrounds the main flexural reinforcement with an Engineered Cementitious Composite (ECC) which exhibits strain-hardening and multiple-cracking behavior under uni-axial tensile loading. This alternate design with layered ECC is referred to in this paper as Functionally-Grade Concrete (FGC).

Maalej and Li (1995) had shown that the maximum crack width in an FGC beam under service load can be limited to values that are very difficult to achieve using conventional steel reinforcement and commonly used concrete. It was suggested that the ECC material in FGC beams could provide two levels of protection. First, it could prevent the migration of aggressive substances into the concrete, therefore, preventing reinforcement corrosion. Second, in the extreme case when corrosion initiates, accelerated corrosion due to longitudinal cracks would be reduced if not eliminated, and spalling and delamination problems common to many of today's RC structures would be prevented. This was expected due to the high strain capacity and fracture resistance of the ECC material.

[1]Assistant Professor, Department of Civil Engineering, National University of Singapore, Singapore.
E-mail: cvemm@nus.edu.sg
[2]Research Scholar, Department of Civil Engineering, National University of Singapore, Singapore.
[3]Professor, Department of Civil Engineering, National University of Singapore, Singapore.

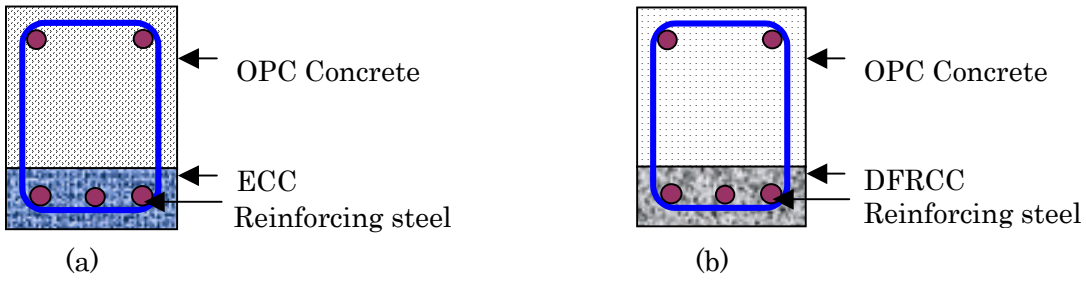

Fig. 1 Concept of functionally-graded concrete (a) Maalej and Li (1995) (b) This investigation.

In this paper, the concept proposed by Maalej and Li (1995) is adopted to prepare a series of FGC beams where a layer of DFRCC material, exhibiting strain-hardening and multiple-cracking behavior under third-point flexural loading, is used around the main longitudinal reinforcement for corrosion protection (**Fig. 1b**). The objective of the study is to evaluate the effectiveness of DFRCC in retarding the corrosion of steel reinforcement in RC beams and reducing the tendency of the concrete cover to delaminate as measured by a concrete-embeddable fiber optic strain sensor (FOSS). The effects of steel loss and corrosion damage on the flexural response of RC beams will also be evaluated.

2. Experimental program

Two series of RC beams are included in the test program (see **Table 1**). The first series consists of two medium-scale conventional RC beams measuring 300 x 210 x 2500 mm (**Fig. 2**). The second series consists of three specimens, which are similar to those in the first series in every aspect, except that the plain concrete that surrounds the tensile steel reinforcement is replaced

Table 1 Summary of experimental program.

Series no	Specimen designation	Use of special layer	Structural testing	FOSS gauge	Accelerated corrosion	Estimated steel loss
1	OPCC-1 (control)	Nil	Yes	No	No	-
	OPCC-2	Nil	Yes	Yes	Yes	10 %
2	FGC-1 (control)	DFRCC	Yes	No	No	-
	FGC-2	DFRCC	Yes	Yes	Yes	6.6%
	FGC-3	DFRCC	Yes	Yes	Yes	10 %

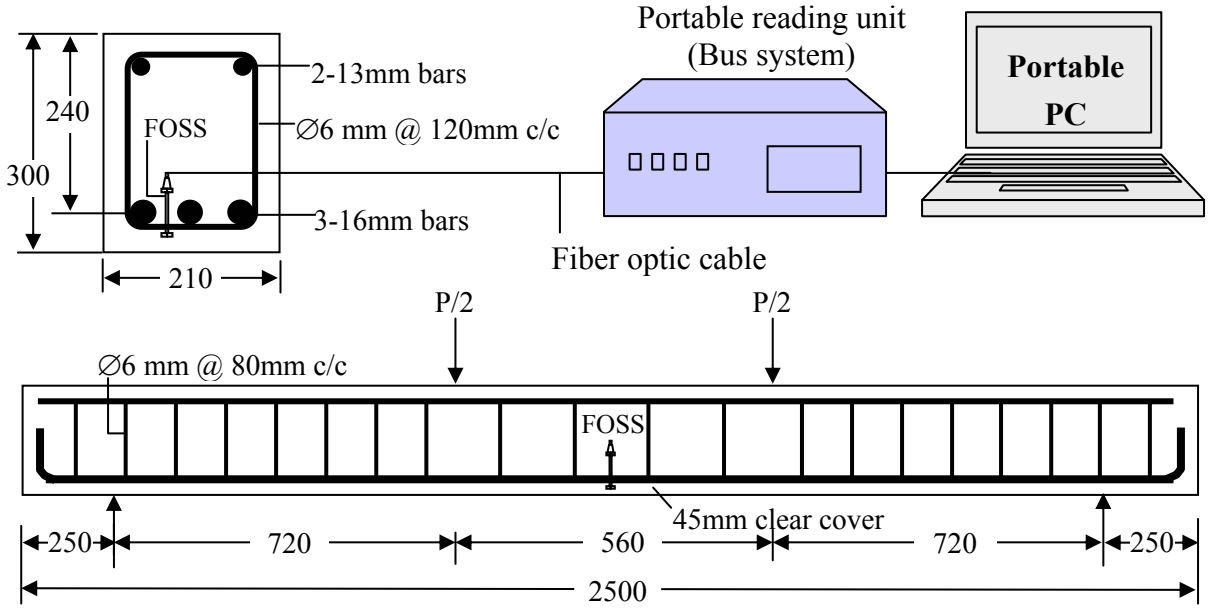

Fig. 2 Details of medium-scale beam specimens (all dimensions in mm).

with an optimized DFRCC made of hybrid fiber reinforced mortar (containing 1% steel and 1.5% PVA fibers). One specimen from the first series (OPCC-2) and two specimens from the second series (FGC-2 and FGC-3) were subjected to accelerated corrosion using a constant-potential electro-chemical technique. The remaining two specimens from each series (OPCC-1 and FGC-1) were kept as control in order to compare their load-deflection behavior with the corroded specimens. The accelerated corrosion of the conventional RC beam (OPCC-2) was terminated when the estimated steel loss reached about 10%. At that time, the accelerated corrosion of one FGC beam (FGC-2) was also terminated. The third FGC specimen (FGC-3) continued undergoing accelerated corrosion until the calculated steel loss reached the target 10%. Corrosion-induced damage in the concrete beams was evaluated by measuring the corrosion current throughout the accelerated corrosion test. In addition, the size and location of cracks were monitored visually and sketched on paper as they appeared. A concrete-embeddable fiber optic strain sensor was used in each corroded beam to measure the corrosion-induced tensile strains in the concrete and the tendency of the concrete cover to delaminate.

All specimens experienced three cycles of loading and unloading up to 70% of their estimated ultimate load prior to undergoing accelerated corrosion. At 70% of the ultimate load, the measured maximum crack widths in specimens OPCC-2, FGC-2 and FGC-3 were 0.54, 0.28 and 0.30 mm, respectively. After unloading, the measured maximum crack widths in the same specimens were 0.19, 0.12 and 0.13 mm, respectively. As expected, the maximum crack widths in the FGC specimens were smaller than those in the OPCC specimens due to the multiple-cracking behavior of the DFRCC material and the bridging effect of the fibers.

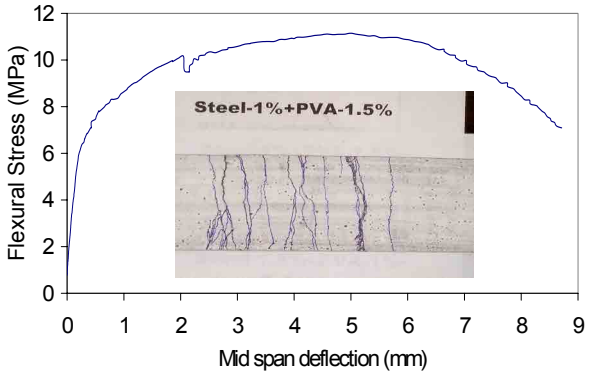

Fig. 3 Flexural response of DFRCC material (Ahmed et al. 2001).

3. Materials

The DFRCC material used in this investigation was reinforced with both high modulus (steel) and low modulus (PVA) fibers with respective volume fractions of 1% and 1.5%. The properties of both fibers are given in **Table 2**. Class F fly ash was used as 50% replacement of ordinary Portland cement in the DFRCC material. The mix proportions of the DFRCC material and the concrete used in this investigation are shown in **Table 3**. The DFRCC material exhibited strain-hardening and multiple-cracking behavior under third-point flexural loading as shown in **Fig. 3** (Ahmed et al. 2001). The measured average ultimate flexural strength, deflection capacity and toughness index were 11.5 MPa, 5 mm and 135, respectively.

The longitudinal reinforcements consisted of 3-16mm diameter deformed bars used in the tension zone and 2-13mm diameter deformed bars used in the compres-

Table 2 Properties of fibers used in DFRCC material.

Fiber type	Length (mm)	Diameter (μm)	Modulus of elasticity (GPa)	Fiber strength (MPa)	Fiber density (gm/cm^3)
Steel	13	160	200	2500	7.8
PVA	12	40	44	1850	1.3

Table 3 Mix proportions and material properties of concrete and DFRCC material.

Mix	Mix proportions (by weight)						Properties	
	Cement	Fly ash	F.A.[a]	C.A.[b]	Water	WRA[c]	28-day compressive strength (MPa)	Resistance to Cl^- penetration (Coulombs)
Concrete	1	-	2	3	0.42	0.005	41.6	4265
DFRCC	0.5	0.5	1	-	0.45	0.020	61.3	2805

[a]F.A.= fine aggregate; [b]C.A. = coarse aggregate; [c]WRA = water reducing admixture.

Table 4 Properties of reinforcing steel.

Property	16mm bar	13mm bar	6mm bar
Yield Stress (MPa)	472	541	366
Ultimate Stress (MPa)	571	561	495
Modulus (GPa)	200	189	211

sion zone, corresponding to reinforcement ratios of 0.96% tensile and 0.44% compressive. Shear reinforcement consisted of 6mm plain bar stirrups spaced at 80 mm in the shear span and 120 mm in the constant moment region. The measured yield strength, ultimate strength and elastic modulus of the longitudinal and transverse reinforcements are shown in **Table 4**.

4. Specimen fabrication

For specimens undergoing accelerated corrosion, the three longitudinal steel bars used in the tension zone were drilled and threaded at each end where electrical wires were connected in order to apply an 8Volt fixed electrical potential for accelerated corrosion. A 250mm long region at both ends of each reinforcement cage was painted with epoxy coating in order to restrict the corrosion within the beam span. Subsequently, the reinforcement cages were placed in their formwork. Plastic chairs, giving 45 mm clear concrete cover were used between the formwork and the reinforcement.

Concrete-embeddable fiber optic strain sensors (**Fig. 4**) were installed in beams OPCC-2, FGC-2 and FGC-3, which were subjected to accelerated corrosion. In each beam, one FOSS gauge was placed vertically between two longitudinal bars at the mid-span as shown in **Fig. 2**. Sufficient care was taken during casting in order to avoid any possible damage to the FOSS gauge during vibration. Casting of the FGC beams (second series) was done in two stages. The DFRCC material was first prepared and poured into the moulds. After about one hour, the plain concrete was prepared and poured on top of the DFRCC layer without any special preparation of the interface between the DRFCC and the plain concrete. After casting, all specimens were wet cured for 28 days.

Fig. 4 Fiber optic strain sensor.

5. Accelerated corrosion and monitoring system

Accelerated corrosion was achieved by subjecting the bottom half of the specimens to cyclic wetting and drying (3.5 days wetting and 3.5 days drying) using water containing 3% (by weight) sodium chloride. In addition, a current was impressed using an 8Volt fixed electrical potential applied across an internal anode (the steel reinforcement) and an external cathode built from a 3mm-diameter wire mesh with 15mm square openings. The applied potential and resulting current values were automatically recorded using a data acquisition system and a personal computer. The measured current was used to estimate the amount of steel loss using Faraday's law:

$$\Delta w = \frac{MIt}{ZF} \tag{1}$$

where Δw = mass of steel loss (grams), I = corrosion current (amperes), t = time (seconds), F = Faraday's constant (96,500 amperes seconds), Z = valency of Fe (2), and M = atomic mass of Fe (56 grams/mole).

Faraday's law was used in several studies to estimate the amount of steel loss in reinforced concrete members due to accelerated corrosion (Hearn and Aiello 1998; Lee 1998; Auyeung et al. 2000; Debaiky et al. 2001). In these studies, theoretical steel losses were based on 100% current efficiency, which means that all of the applied current was used in the dissolution of iron. However, Auyeung et al. (2000) argued that a certain amount of energy was needed to initiate corrosion of steel reinforcement embedded in concrete. As a result, calculated steel losses tended to overestimate actual losses. In their study, the correlation between calculated steel loss and actual steel loss was according to the following relationship:

$$\text{actual mass loss} = 0.465\ \text{theoretical mass loss} - 0.562 \tag{2}$$

Auyeung et al. (2000) also observed that higher concrete compressive strength (or lower concrete permeability) led to less corrosion than predicted. In addition, it was observed that the presence of corrosion-induced cracks reduced the discrepancy between calculated and actual steel losses. As will be discussed later, these observations are important in the interpretations of tests results obtained from the current study.

6. Monitoring corrosion damage using fiber optic sensing technique

In this study, a concrete-embeddable fiber optic strain sensor (Fabry-Perot type) was used to monitor the corrosion-induced tensile strain in the concrete at the level of longitudinal tension reinforcement where splitting cracks are likely to occur (see **Figs. 5** and **6**). The Fabry-Perot strain gauge itself is bonded in a very small diameter longitudinal hole located in the center of a concrete-embeddable stainless steel body measuring 70mm in length and having two flanges at both ends for better adherence to concrete. The advantage of this fiber optic strain sensor over its conventional counterparts is that it provides stable absolute measurement of strain needed in experiments involving long-term monitoring. Fiber optic cables connect the sensors to a four-channel portable reading unit (called Bus system). Data from three channels used in this experiment were read simultaneously and stored by a data acquisition software in a personal computer.

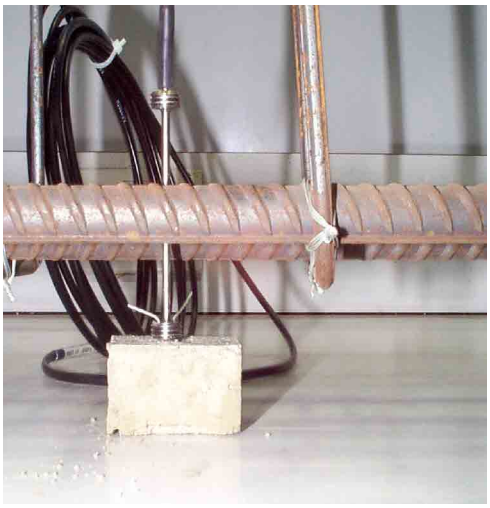

Fig. 5 FOSS between longitudinal bars.

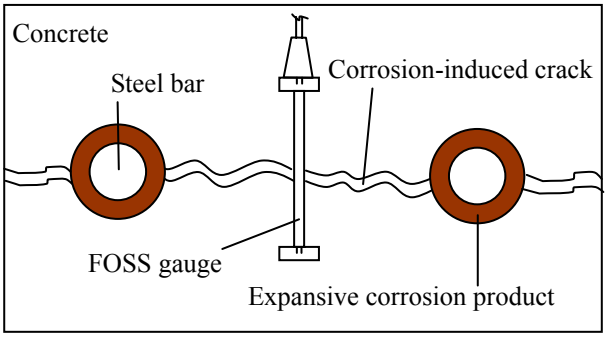

Fig. 6 Concept of using FOSS gauge to measure corrosion-induced damage.

7. Post-corrosion chloride content and pH values

At the end of the accelerated corrosion test, powder samples were collected from all beams at the level of reinforcing steel in order to determine the chloride content and pH value of the concrete and the DFRCC material. In the determination of chloride content, BS 1881: Part 124 (1988) was followed. To determine the pH value, a procedure similar to that used by Lorentz and French (1995) was followed, where the collected powder samples were mixed with 50 ml of de-ionized water. A pH meter was later used to measure the pH of the prepared solution. In each case, six readings were taken and averaged to obtain the pH value of a given solution. After each reading, the electrode of the pH meter was washed with de-ionized water and the calibration of pH meter was checked with standard buffer solution.

8. Test results and discussions

The compressive strength and the resistance to chloride-ion penetration of the OPC concrete and the DFRCC material are shown in **Table 3**. The DFRCC material showed a higher resistance to chloride-ion penetration than the OPC concrete as indicated by the ASTM C 1202 test (1997).

8.1 Corrosion resistance of FGC concrete beams

The conventional RC specimen OPCC-2 lost an estimated 10.1% of its steel reinforcement in about 83 days. During the same accelerated corrosion period, the FGC specimen FGC-2 lost an estimated 6.6% of its steel reinforcement. The better corrosion resistance (measured in terms percentage steel loss) of specimen FGC-2 is also consistent with the rapid chloride permeability test (RCPT) results shown in **Table 3** as well as the post-corrosion chloride content and the pH values of powder samples shown in **Table 5**. Specimen FGC-3, on the other hand, took about 141 days to reach the target 10 % calculated steel loss. The longer time required by specimen FGC-3 to reach the same level of calculated steel loss as specimen OPCC-2 is probably due to the higher resistance of the DFRCC material to chloride-ion penetration as well as the higher compressive strength (or lower permeability) of DFRCC and the absence of corrosion-induced cracking in the FGC beams.

8.2 Foss readings

Figure 7 shows the variation of concrete strain as measured by the FOSS gauges over time. During the first 27 days, the FOSS strain in specimen OPCC-2 was slightly higher than those in specimens FGC-2 and FGC-3 and can be attributed to the higher rate of steel loss in the former beam compared to the latter ones. The measured strain in specimen OPCC-2 increased suddenly after about 27 days as shown in **Fig. 7** and a lon-

Table 5 Summary of post-corrosion test results.

Specimen designation	Yield load (kN)	Peak load (kN)	Load at failure[a]		Deflection at failure[a]		Average corr. current (amps)		Steel loss[b] (%)	Chloride content (%)	pH value
			(kN)	% of control	(mm)	% of control	Wet cycle	Dry cycle			
OPCC-1	201.9	208.2	197.7	-	26.1	-	-	-	-	0.014	12.9
OPCC-2	167.1	181.1	171.4	87	21.1	91	1.06	0.07	10.1	0.46	11.6
FGC-1	234.7	239.6	226.3	-	29.8	-	-	-	-	0.01	12.7
FGC-2	224.4	227.0	215.6	95	29.8	100	0.81	0.05	6.6	0.09	12.1
FGC-3	207.6	213.0	202.0	89	28.0	94	0.65	0.03	10.0	0.14	11.9

[a]beams are considered to have failed once the applied load drops to about 95 percent of the peak load.
[b]based on Faraday's law.

gitudinal crack formed at that time. The strain in beam OPCC-2 continued to increase with the progress of corrosion and the highest recorded FOSS reading was about 1686 microstrains. On the other hand, the rates of FOSS strain increase in both specimens FGC-2 and FGC-3 continued to be very low during the accelerated corrosion regime and the highest recorded FOSS readings were 277 and 442 for specimens FGC-2 and FGC-3, respectively. Therefore, there was no sudden increase in FOSS strain recorded in the FGC specimens as there was no corrosion-induced cracks that had developed in either beam. The low FOSS readings and the absence of corrosion-induced cracks in the FGC specimens are probably due to the higher tensile strain capacity and fracture resistance of the DFRCC material compared to OPC concrete. The fibers in the DFRCC material suppress the growth of cracks and prevent strain localization resulting is specimens that are free from corrosion–induced cracking.

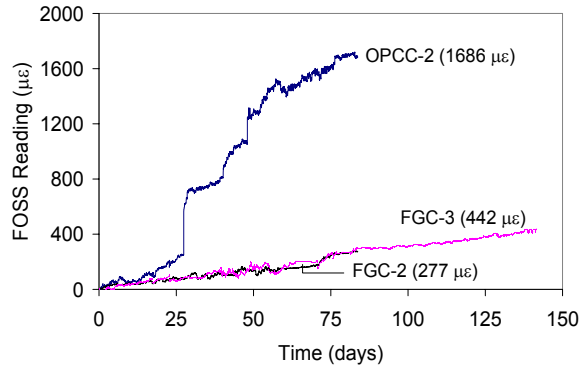

Fig. 7 Corrosion-induced tensile strain in concrete as measured by FOSS gauge.

8.3 Crack mapping

Throughout the accelerated corrosion process, the size and location of cracks were sketched on paper as they appeared (**Fig. 8**). In the case of specimen OPCC-2, longitudinal cracks followed by some branch cracks formed on both sides of the beam along the tension reinforcement. Cracks along the stirrups were also noticed in the bottom half of the beam where cracking was generally most extensive. As for the FGC beams, however, no longitudinal cracks were observed as expected. Instead, leaching of soft corrosion products from few points along the interface between the concrete and the DFRCC layer were noticed in both beams. These were believed to be associated with limited corrosion of the stirrups at these locations. The observed corrosion spots on both FGC beams are shown in **Fig. 8b**.

8.4 Structural testing of beams

Both corroded and uncorroded beams were tested under four-point loading as shown in **Fig. 2**. The load was applied under displacement control at a loading rate of 0.010mm/sec using a universal testing machine with a maximum capacity of 500 kN. A total of 3 LVDTs were

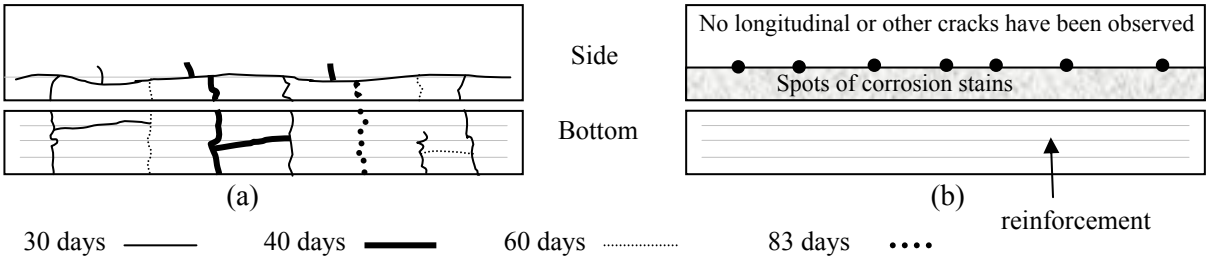

Fig. 8 Progress of corrosion damage according to specified time intervals.
(a) OPCC-2 Beam (b) FGC-2 and FGC-3 beams.

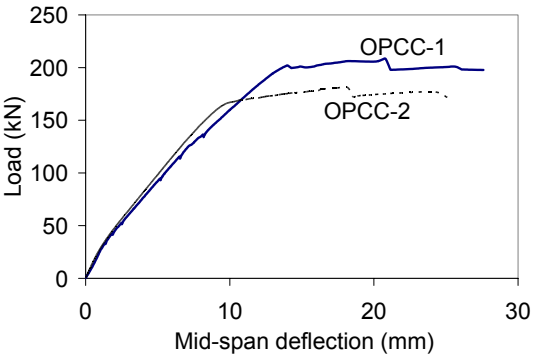

(a)

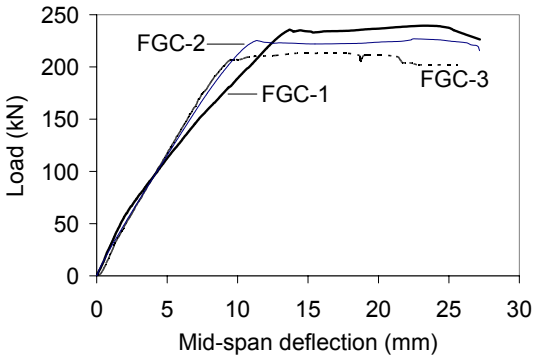

(b)

Fig. 9 Load-deflection response of un-corroded and corroded beams (a) OPCC beams (b) FGC beams.

used to measure the mid-span and load-line deflections of the beams during testing.

The load-deflection responses for all corroded and uncorroded RC beams are shown in **Fig. 9** and summarized in **Table 5**. **Figure 9a** shows the load-deflection curves for the corroded and uncorroded OPC concrete beams. As the figure shows, the corroded beam (OPCC-2) lost about 13% of its ultimate load-carrying capacity and 9% of its deflection capacity. In the corroded specimen, after reaching the yield load, a longitudinal crack which had originally formed during the accelerated corrosion test continued to increase in width as the load continued to increase. That led to slight delamination of the concrete cover upon reaching the peak load and cover spalling at failure as shown in **Fig. 10a-10b**.These finding are consistent with results from previous studies (Umoto and Misra 1998; Mangat and Elgarf 1999; Bonacci and Maalej 2000) reporting reductions in the flexural load capacity and deflection of ordinary RC beams due to reinforcement corrosion. In these studies, breakdown of the bond at the concrete-steel interface and corrosion-induced cracking were identified as the primary cause of loss of strength and ductility.

Figure 9b shows the load-deflection curves for the FGC specimens. **Figure 9b** and **Table 5** indicate that specimen FGC-2 lost about 5% of its load capacity at failure due to accelerated corrosion. However, its deflection capacity at failure was essentially not affected. Specimen FGC-3, on the other hand, lost 11% of its load capacity and 6% of its deflection capacity at failure. This specimen was subjected to accelerated corrosion for a longer period of time and lost a higher percentage of its internal steel reinforcement (compared to specimen FGC-2). By looking at the cracking patterns during structural testing in all specimens, it was noticed that the FGC specimens had about twice the number of load-induced cracks as those in the OPCC specimens (**Fig. 11**). This may be attributed to the strain-hardening and multiple-cracking behavior of the DFRCC material used in the FGC specimens. However, no sign of delamination of the concrete cover or between the concrete and the DFRCC layer was observed in the FGC

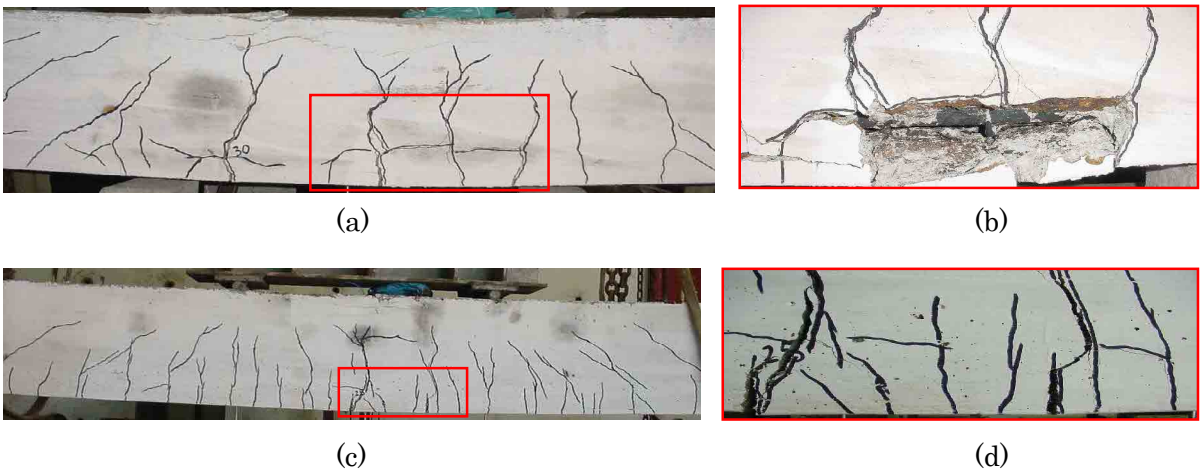

(a) (b) (c) (d)

Fig. 10 Typical cracking patterns of corroded beams (a) OPCC-2 at about peak load; (b) Close-up of region highlighted in (a) after failure; (c) FGC-3 at about peak load; (d) Close-up of region highlighted in (c) after failure.

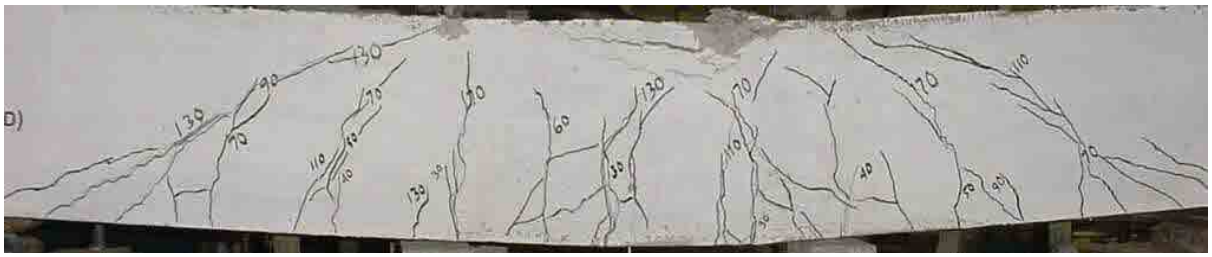

(a)

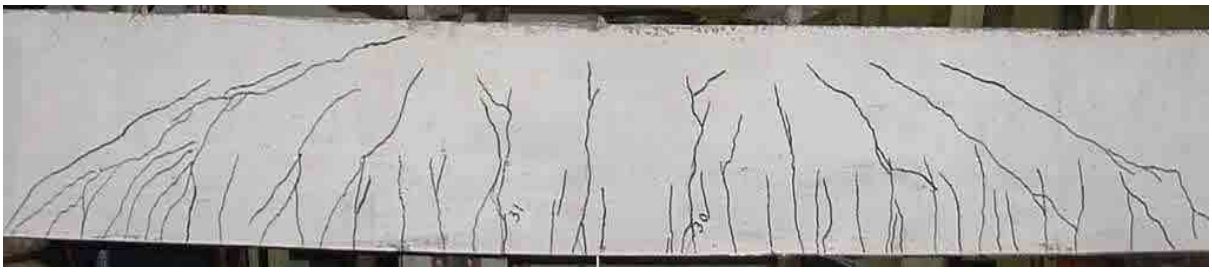

(b)

Fig. 11 Cracking patterns of un-corroded beams at ultimate load (a) OPCC-1 (b) FGC-1.

specimens during structural testing.

Concrete is known to be weak in tension and corrosion products require about 2-3 times the volume of the original steel lost to corrosion (Beeby 1978). This means that in a conventional RC beam, in addition to the loss of steel section, corrosion-induced cracks will develop leading to, among other things, delamination and loss of bond between the concrete and the steel rebar (Al-Sulaimani et al 1990). This may explain the observed loss of load and deflection capacities observed in specimen OPCC-2. The scenario is quite different in the FGC specimens. Although the loss of steel section can still take place, particularly when the corrosion is induced, the damage to the steel/DFRCC material interfacial bond is probably quite low due to a potentially high tensile strain capacity of the DFRCC material. Moreover, the fibers in the DFRCC material can effectively bridge the cracks, thus improving the confining and holding capacity of the surrounding DFRCC material to the steel bar resulting in minimum loss of bond due to corrosion. This may explain why the FGC specimens have retained most of original deflection capacity despite undergoing accelerated corrosion.

8.5 Examination of the distribution of steel loss

After structural testing, part of the concrete cover in specimen OPCC-2 was removed to expose the reinforcing bars and the stirrups and examine the extent and the uniformity of the steel loss. The examination revealed a fairly uniform loss of steel along the longitudinal and the transverse reinforcement as shown in **Fig. 12a**. Few spots of pitting corrosion have also been observed on both the longitudinal and the transverse reinforcement.

With significant difficulty, part of the concrete cover of specimen FGC-3 was also removed to expose the reinforcing steel for examination. The examination revealed a minimum loss of steel in the longitudinal reinforcement (**Fig. 12b**), except for the mid-span region where the load-induced pre-cracks were largest in width. In this region, moderate loss of steel could be observed, but there was no evidence for the presence of corrosion-induced radial cracks or delamination around the longitudinal reinforcing bars. As for the stirrups, there was evidence of some pitting corrosion at the interface between the concrete and the DFRCC material, and these must have been the source of the corrosion spots observed at these locations. This pitting corrosion, however, did not seem to affect the load-deflection behavior of the beam given the fact that the RC beams were not shear critical.

Although according to Faraday's law, both specimens OPCC-2 and FGC-3 have undergone the same amount of steel loss, **Fig. 12** clearly indicates that the steel loss in the FGC specimen is generally very limited. This difference may be due to two main reasons. Firstly, while Faraday's law is known to overestimate the actual steel loss, in light of the finding reported by Auyeung et al. (2000), it is believed that in the case of the FGC beams, which have higher compressive strength and likely lower permeability and where no corrosion-induced cracks have been observed, Faraday's law grossly overestimate the actual amount of steel loss in the FGC beams in comparison to the OPCC beams. Secondly, because the DFRCC material in the FGC beams offered the longitudinal reinforcement high protection against reinforcement corrosion, most of the corrosion activities shifted to the stirrups in the bottom half of the beam just above the DFRCC layer.

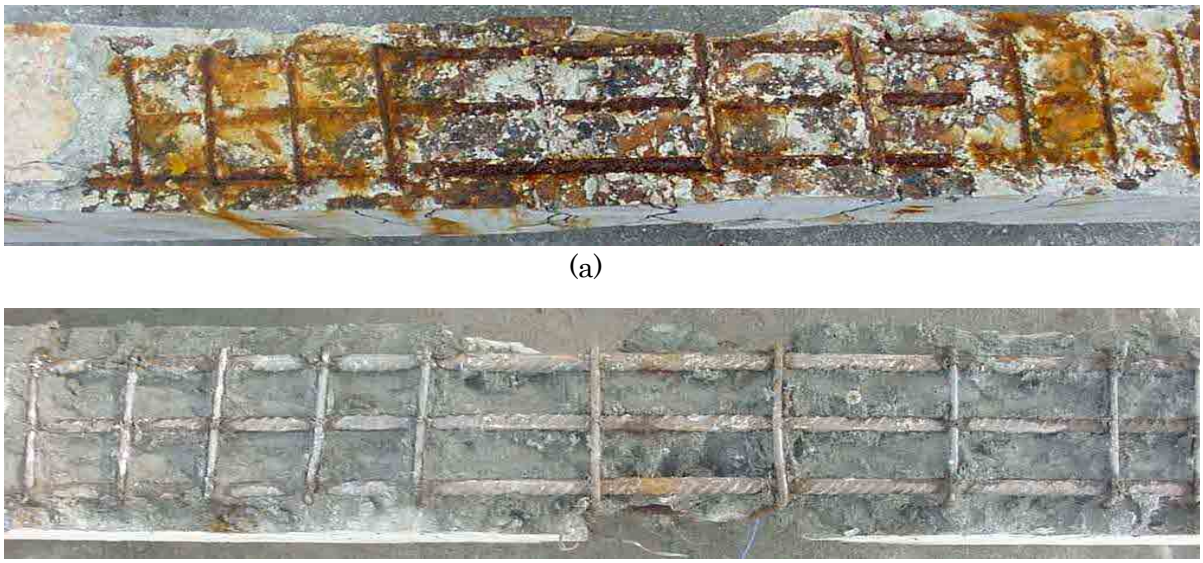

(a)

(b)

Fig. 12 Corrosion status of steel in (a) OPCC-2 beam and (b) FGC-3 beam.

9. Conclusions

The resistance of FGC beams to corrosion and corrosion-induced damage and the structural response of FGC beams subjected to accelerated corrosion were evaluated experimentally in this study. At any given time, the FGC beams were found to exhibit lower level of steel loss than the OPCC beam. It was also observed that an FGC beam takes about 70% longer time to achieve the same level of calculated steel loss compared to an OPCC beam. This percentage would be even higher if the comparison was based on actual steel loss. The better performance of the FGC beams over the OPCC beam was also evident from the absence of any corrosion-induced cracks or damage and the lowest tendency for the concrete cover to delaminate as measured by a concrete-embeddable FOSS. For the same level of calculated steel loss, an FGC specimen exhibited higher residual load and deflection capacities compared to its OPCC counterpart. While a corroded OPCC beam was found to experience widening of corrosion-induced cracks, delamination and spalling during loading, no such behavior was observed in the FGC beams. The FGC concept using DFRCC material was found in this study to be very effective in preventing corrosion-induced damage in RC beams and minimizing the loss in the beam's load and deflection capacities. These positive results, obtained from laboratory tests under very simplified idealization of the field conditions, warrant further tests on the corrosion durability and structural response of functionally-graded concrete beams.

Acknowledgements

The authors would like to acknowledge the Kuraray Co. Ltd. of Japan, Bekaert Co. Ltd. of Belgium and National Cement Co. Ltd. of Singapore for supplying PVA fibers, steel fibers and fly ash, respectively. Part of this research was supported by a research grant (R-264-000-105-112) from the National University of Singapore. Helpful comments from three anonymous reviewers led to improvement of the manuscript and are gratefully acknowledged.

References

ACI Committee 224 (1991). "*Control of cracking in concrete structures*." ACI Manual of Concrete Practice Part 3-1991: Use of Concrete in Buildings—Design, Specifications, and Related Topics, *American Concrete Institute*, Detroit, USA.

ACI Committee 318-99 (1999). "*Building code requirements for reinforced concrete (ACI 318-99) and commentary (ACI 318R-99)*." American Concrete Institute, Detroit, USA.

Ahmed, S. F. U., Maalej, M. and Paramasivam, P. (2001). "Strain-hardening behaviour of hybrid fibre reinforced cement composites." *Proceedings of Seventh International Symposium on Ferrocement and Thin Reinforced Cement Composites*, Ed. Mansur, M. A. and Ong, G., Singapore, 215-226.

Al-Sulaimani, G. J., Kaleemullah, M., Basunbul, I. A. and Rasheeduzzafar. (1990). "Influence of corrosion and cracking on bond behavior and strength of reinforced concrete members." *ACI Structural Journal*, 87 (2), 220-231.

ASTM C 1202-97 (1997). "*Standard test method for*

electrical indication of concrete's ability to resist chloride ion penetration." American Society for Testing and Materials, Pennsylvania, USA.

Auyeung, Y., Balaguru, P. and Chung, L. (2000). "Bond behavior of corroded reinforcement bars." *ACI Materials Journal*, 97 (2), 214-220.

Beeby, A. W. (1978). "Corrosion of reinforcing steel in concrete and its relation to cracking." *Structural Engineer*, 56A (3), 77-81.

Bonnaci, J. F. and Maalej, M. (2000). "Externally bonded FRP for rehabilitation of corrosion damaged concrete beams." *ACI Structural Journal*, 97 (5), 703-711.

BS 1881: Part 124 (1988). "*Standard test method for determination of chloride content in the concrete*." British Standards Institution, London, UK.

CANMET (1987). "*Supplementary cementing materials for concrete*." ed. V.M. Malhotra, CANMET, Canada.

CEB (1993). "*CEB-FIP model code 1990: design code.*" Comité Euro-International du Béton, Thomas Telford, London, UK.

Debaiky, A. S., Green M. F. and Hope, B. B. (2001). "Corrosion of FRP-wrapped RC cylinders—long term study under severe environmental exposure." *Proceedings of the 5th International Conference on Fibre Reinforced Polymers for Reinforced Concrete Structures*, Cambridge, England, 1073-1082.

Hearn, N. and Aiello, J. (1998). "Effect of mechanical restraint on the rate of corrosion in concrete." *Canadian Journal of Civil Engineering*, 25 (1), 81-86.

Lee, C. (1998). "*Accelerated corrosion and repair of RC columns using CFRP sheets*." M. A. Sc. Thesis, Department of Civil Engineering, University of Toronto, Canada.

Lorentz, T. and French, C. (1995). "Corrosion of reinforcing steel in concrete: effects of materials, mix composition and cracking." *ACI Materials Journal*, 92 (2), 181-190.

Maalej, M. and Li, V. C. (1995). "Introduction of strain hardening engineered cementitious composites in design of reinforced concrete flexural members for improved durability." *ACI Structural Journal*, 92 (2), 167-176.

Mangat, P. S. and Elgarf, M. S. (1999). "Flexural strength of concrete beams with corroding reinforcement." *ACI Structural Journal*, 96 (1), 149-158.

Mehta, P. K. (1998). "Role of pozzolanic and cementitious materials in sustainable development of the concrete industry." *Proceedings of sixth CANMET/ACI Conference*, Ed. Malhotra, V. M., ACI SP-178, 1-20.

Mehta, P. K. (1999). "Advancements in concrete technology." *Concrete International*, 21 (6), 69-75.

Tsukamoto, M. and Worner, J. D. (1990). "Tightness of fiber concrete." *Darmstadt Concrete, Annual Journal on Concrete and Concrete Structures,* 5, 215-225.

Umoto, T. and Misra, S. (1998). "Behavior of concrete beams and columns in marine environment when corrosion of reinforcing bars takes place." *Proceedings of the Second International Conference on Concrete in Marine Environment,* Ed. Malhotra, V. M., Canada, 127-146.